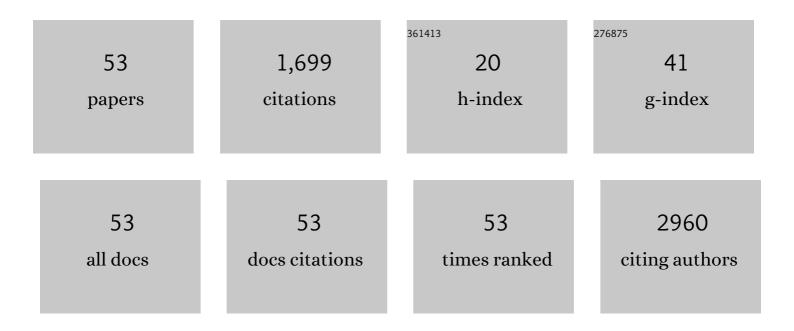
Ansoon Kim

List of Publications by Year in descending order

Source: https://exaly.com/author-pdf/3689720/publications.pdf Version: 2024-02-01



ANSOON KIM

#	Article	lF	CITATIONS
1	Ultrasensitive, label-free, and real-time immunodetection using silicon field-effect transistors. Applied Physics Letters, 2007, 91, .	3.3	229
2	Ambient Pressure Syntheses of Size-Controlled Corundum-type In2O3Nanocubes. Journal of the American Chemical Society, 2006, 128, 9326-9327.	13.7	185
3	Hot-Spot Engineering in Polygonal Nanofinger Assemblies for Surface Enhanced Raman Spectroscopy. Nano Letters, 2011, 11, 2538-2542.	9.1	180
4	Melamine Sensing in Milk Products by Using Surface Enhanced Raman Scattering. Analytical Chemistry, 2012, 84, 9303-9309.	6.5	167
5	Study of Molecular Trapping Inside Gold Nanofinger Arrays on Surface-Enhanced Raman Substrates. Journal of the American Chemical Society, 2011, 133, 8234-8239.	13.7	103
6	SERS-based pesticide detection by using nanofinger sensors. Nanotechnology, 2015, 26, 015502.	2.6	79
7	Direct label-free electrical immunodetection in human serum using a flow-through-apparatus approach with integrated field-effect transistors. Biosensors and Bioelectronics, 2010, 25, 1767-1773.	10.1	77
8	Enhanced Protein Immobilization Efficiency on a TiO ₂ Surface Modified with a Hydroxyl Functional Group. Langmuir, 2009, 25, 11692-11697.	3.5	45
9	Absolute work function measurement by using photoelectron spectroscopy. Current Applied Physics, 2021, 31, 52-59.	2.4	45
10	Response to Cardiac Markers in Human Serum Analyzed by Guided-Mode Resonance Biosensor. Analytical Chemistry, 2010, 82, 9686-9693.	6.5	44
11	Gadolinium Oxide Nanoring and Nanoplate:  Anisotropic Shape Control. Crystal Growth and Design, 2007, 7, 1378-1380.	3.0	42
12	Fabrication of Deterministic Nanostructure Assemblies with Sub-nanometer Spacing Using a Nanoimprinting Transfer Technique. ACS Nano, 2012, 6, 6446-6452.	14.6	42
13	Dissociative Chemisorption of Methanol on Ge(100). Journal of Physical Chemistry C, 2007, 111, 15013-15019.	3.1	37
14	Elasticity-based development of functionally enhanced multicellular 3D liver encapsulated in hybrid hydrogel. Acta Biomaterialia, 2017, 64, 67-79.	8.3	34
15	Heterojunction solar cell based on n-MoS2/p-InP. Optical Materials, 2018, 86, 576-581.	3.6	32
16	Phase-Selective Disordered Anatase/Ordered Rutile Interface System for Visible-Light-Driven, Metal-Free CO ₂ Reduction. ACS Applied Materials & Interfaces, 2019, 11, 35693-35701.	8.0	32
17	Highly sensitive detection of cardiac troponin I in human serum using gold nanoparticle-based enhanced sandwich immunoassay. Sensors and Actuators B: Chemical, 2015, 221, 537-543.	7.8	28
18	Energy gap modulation in V2O5 nanowires by gas adsorption. Applied Physics Letters, 2008, 93, .	3.3	27

ANSOON KIM

#	Article	IF	CITATIONS
19	Bidentate Structures of Acetic Acid on Ge(100):  The Role of Carboxyl Oxygen. Journal of Physical Chemistry C, 2007, 111, 5941-5945.	3.1	23
20	lonic Current Rectification of Porous Anodic Aluminum Oxide (AAO) with a Barrier Oxide Layer. ACS Nano, 2020, 14, 13727-13738.	14.6	22
21	Observation of temperature-dependent kinetics for catalytic CO oxidation over TiO2-supported Pt catalysts. Chemical Physics Letters, 2017, 685, 282-287.	2.6	21
22	Thermal annealing of black phosphorus for etching and protection. Applied Surface Science, 2018, 457, 773-779.	6.1	17
23	Control of channel doping concentration for enhancing the sensitivity of †top-down' fabricated Si nanochannel FET biosensors. Nanotechnology, 2009, 20, 475501.	2.6	15
24	Band engineering of a Si quantum dot solar cell by modification of B-doping profile. Solar Energy Materials and Solar Cells, 2017, 159, 80-85.	6.2	14
25	Fabrication of Anionic Sulfate-Functionalized Nanoparticles as an Immunosensor by Protein Immobilization. Langmuir, 2010, 26, 7355-7364.	3.5	13
26	Photosensitive biosensor array system using optical addressing without an addressing circuit on array biochips. Applied Physics Letters, 2010, 97, .	3.3	11
27	Quantitative analysis of Si1-xGex alloy films by SIMS and XPS depth profiling using a reference material. Applied Surface Science, 2018, 432, 72-77.	6.1	11
28	Discrimination of Chiral Adsorption Configurations: Styrene on Germanium(100). Journal of Physical Chemistry C, 2009, 113, 1426-1432.	3.1	10
29	Improved electrical properties of silicon quantum dot layers for photovoltaic applications. Solar Energy Materials and Solar Cells, 2016, 150, 71-75.	6.2	10
30	Enhancement of Photoresponse on Narrow-Bandgap Mott Insulator α-RuCl ₃ <i>via</i> Intercalation. ACS Nano, 2021, 15, 18113-18124.	14.6	10
31	Nanogap Array Fabrication Using Doubly Clamped Freestanding Silicon Nanowires and Angle Evaporations. ETRI Journal, 2009, 31, 351-356.	2.0	9
32	Efficiency improvement of Si quantum dot solar cells by activation with boron implantation. Solar Energy, 2018, 164, 89-93.	6.1	9
33	Atomic Layer MoS2xTe2(1–x) Ternary Alloys: Two-Dimensional van der Waals Growth, Band gap Engineering, and Electrical Transport. ACS Applied Materials & Interfaces, 2020, 12, 40518-40524.	8.0	8
34	The role of active species in the N 2 and N 2 -H 2 RF afterglows on selective surface nitriding of ALD-grown TiO 2 films. Surface and Coatings Technology, 2017, 324, 243-248.	4.8	7
35	Modified ion sensitive field effect transistor sensors having an extended gate on a thick dielectric. Applied Physics Letters, 2010, 96, 203702.	3.3	6
36	Analysis of configuration of surface-immobilized proteins by Si nanochannel field effect transistor biosensor. Sensors and Actuators B: Chemical, 2011, 154, 164-168.	7.8	6

ANSOON KIM

#	Article	IF	CITATIONS
37	Self-Heating-Induced Deterioration of Electromechanical Performance in Polymer-Supported Metal Films for Flexible Electronics. Scientific Reports, 2017, 7, 12506.	3.3	6
38	Photo selective protein immobilization using bovine serum albumin. Applied Surface Science, 2012, 261, 880-889.	6.1	5
39	Ultraviolet responses of a heterojunction Si quantum dot solar cell. Nanotechnology, 2017, 28, 035402.	2.6	5
40	A study on selective surface nitridation of TiO 2 nanocrystals in the afterglows of N 2 and N 2 -O 2 microwave plasmas. Applied Surface Science, 2018, 432, 163-169.	6.1	5
41	Biosensors using the Si nanochannel junction-isolated from the Si bulk substrate. Journal of Applied Physics, 2009, 106, 114701.	2.5	4
42	Colorimetric Analysis on Flocculation of Bioinspired Au Self-Assembly for Biophotonic Application. Journal of Nanomaterials, 2009, 2009, 1-6.	2.7	4
43	Deterministic nanoparticle assemblies: from substrate to solution. Nanotechnology, 2014, 25, 155302.	2.6	4
44	A spontaneous change in the oxidation states of Pd/WO3 toward an active phase during catalytic cycles of CO oxidation. Surface Science, 2017, 665, 43-50.	1.9	4
45	The role of hydrogen in the nitriding of anatase TiO2 films in the N2-H2 microwave afterglows. Surface and Coatings Technology, 2019, 364, 341-346.	4.8	4
46	Configuration Specific Desorption by Scanning Tunneling Microscope in Organic-Semiconductor Hybrid Systems. Journal of Physical Chemistry C, 2008, 112, 1493-1497.	3.1	3
47	Analysis of configuration of surface-immobilized proteins by Si nanochannel field effect transistor biosensor. Procedia Chemistry, 2009, 1, 674-677.	0.7	2
48	Comparative Study of Silicon Quantum Dot Formation In-situ Grown with a Gas Mixture of SiH4+N2 and SiH4+NH3. Journal of the Korean Physical Society, 2011, 59, 308-311.	0.7	2
49	Controlling N and C-atom densities in N2/H2 and N2/CH4 microwave afterglows for selective TiO2 surface nitriding. Applied Surface Science, 2021, 540, 148348.	6.1	1
50	Modified ISFETs having an extended gate on the thick dielectric. , 2009, , .		0
51	Hybrid gold nanofinger SERS structure for sensing applications. Materials Research Society Symposia Proceedings, 2011, 1359, 141.	0.1	0
52	Selective transfer of nanostructured assemblies onto an arbitrary substrate by nanoimprinting. Proceedings of SPIE, 2012, , .	0.8	0
53	Unexpected Chemical and Thermal Stability of Surface Oxynitride of Anatase TiO2 Nanocrystals Prepared in the Afterglow of N2 Plasma. Applied Science and Convergence Technology, 2017, 26, 62-65.	0.9	0